SELECTED PAPERS FROM IEEE/CIC ICCC 2018

Cross-Layer Framework for Capacity Analysis in Multiuser Ultra-Dense Networks with Cell DTx

Qing Li[1], Yu Chen[1,*], Qimei Cui[1,*], Yu Gu[1], Guoqiang Mao[2]

[1] National Engineering Laboratory for Mobile Network Technologies, Beijing University of Posts and Telecommunications, Beijing 100876, China

[2] School of Computing and Communications, University of Technology Sydney, NSW 2007, Australia

* The corresponding authors, emails: yu.chen@bupt.edu.cn, cuiqimei@bupt.edu.cn

Abstract: Cell discontinuous transmission (Cell DTx) is a key technology to mitigate inter-cell interference (ICI) in ultra-dense networks (UDNs). The aim of this work is to understand the impact of Cell DTx on physical-layer sum rates of SBSs and link-layer quality-of-service (QoS) performance in multiuser UDNs. In this work, we develop a cross-layer framework for capacity analysis in multiuser UDNs with Cell DTx. In particular, we first extend the traditional one-dimensional effective capacity model to a new multidimensional effective capacity model to derive the sum rate and the effective capacity. Moreover, we propose a new iterative bisection search algorithm that is capable of approximating QoS performance. The convergence of this new algorithm to a unique QoS exponent vector is later proved. Finally, we apply this framework to the round-robin and the max-C/I scheduling policies. Simulation results show that our framework is accurate in approximating 1) queue length distribution, 2) delay distribution and 3) sum rates under the above two scheduling policies, and further show that with the Cell DTx, systems have approximately 30% higher sum rate and 35% smaller average delay than those in full-buffer scenarios.

Keywords: effective capacity; QoS performance; sum rates; multiuser scheduling; ultra-dense network (UDN)

Received: Feb. 20, 2019
Revised: Mar. 25, 2019
Editor: Zhiyong Feng

I. INTRODUCTION

Ultra-dense Networks (UDNs) is a key technology in 5G systems to achieve the 1000 fold network capacity increment [1]. As small base stations (SBSs) are densely deployed and operating in the same frequency spectrum [2], severe inter-cell interference (ICI) is introduced, which degrades network performance. Due to the bursty nature of traffic arrival, SBSs may have no data to transmit for a short period [3]. Cell discontinuous transmission (Cell DTx) allows SBSs to be switched to an idle mode in these periods to reduce ICI as well as transmission power [4]. In the downlink transmission, multiple user equipment (UEs) are allowed to share a channel by applying a specific scheduling policy [5]. On the other hand, thanks to the wide usage of real-time services like video-streaming application and V2V communication, meeting the stringent requirements of quality of service (QoS) has become another challenge for 5G systems [6]. Therefore, it is important to understand the

impact of Cell DTx on both sum rates of SBSs and link-layer QoS performance of multiuser UDNs.

A number of work has studied Cell DTx performance in improving the physical-layer spectral efficiency (SE) and energy efficiency (EE). Bonnefoi et al. [7] developed a sub-optimal resource allocation algorithm to minimize the power consumption with DTx. Chang et al. [8] considered the impact of network traffic load on SE and EE. Andersson et al. [9] evaluated the performance of DTx in reducing power consumption under different network deployments. Holtkamp et al. [10] proposed a resource management method to optimize the trade-off between antenna adaptation, power control and DTx in multiuser MIMO-OFDM networks. Polignano et al. [11] studied the impact of DTx on the QoS performance of Voice over IP traffic under dynamic and semi-persistent packet scheduling strategies by simulations. However, these work didn't mathematically analyze the link-layer QoS performance, such as queue length distribution and delay distribution.

QoS performance can be studied by adopting a cross-layer effective capacity model [12]-[14]. Balasubramanian et al. [15] proposed the optimal scheduling scheme to maximize the total system effective capacity. Wang et al. [16] developed an iterative algorithm to find delay-constrained sub-optimal link scheduling strategy in wireless sensor network. In full-buffer scenarios, Weyres et al. [17] analyzed the effective capacity in multiuser networks under the round-robin (RR) and the max-C/I scheduling policies. Cui et al. [18] analyzed networks using both licensed and unlicensed spectrum and calculated the maximum data rate of a link under QoS constraints. Gu et al. [19] considered the burstiness of traffic in UDNs and derived the effective capacity of UDNs in single-user scenarios. However, the above work didn't jointly consider Cell DTx and multiuser scenarios.

In this paper, we continue the work [19] to study multiuser UDNs with Cell DTx and quantitatively analyze sum rates of SBSs and link-layer QoS performance. In summary, we develop a new cross-layer framework that consists of a new multidimensional effective capacity model and a new iterative bisection search algorithm for QoS performance analysis. Part of this work has been published in 2018 IEEE/CIC International Conference on Communications in China (ICCC) [20]. The main contributions of this journal paper include:

- Extension to *N*-SBS Cases: We extend our research to networks with more than two SBSs and develop a cross-layer model to derive distributions of UEs' signal-to-interference-plus-noise ratio (SINR), sum rate in a specific SBS and UEs' effective capacity. Moreover, several properties of the effective capacity are then revealed to further study the network QoS performance;
- A new algorithm: Based on the above properties, we further propose a new iterative bisection search algorithm to approximate the link-layer QoS performance. The convergence of the proposed algorithm to the unique QoS exponent vector is proved through mathematical analysis.
- Application of the framework: We apply this framework to multiuser UDN scenarios under the RR and the max-C/I scheduling policies. The accuracy of our framework is validated as the analytical and simulation results are in a good agreement. The simulations also show that with the Cell DTx, systems have approximately 30% higher sum rate and 35% smaller average delay than those in full-buffer scenarios.

The rest of this paper is organized as follows: Section II explains the system model of multiuser UDNs with Cell DTx. Preliminaries on the traditional effective capacity model is given in Section III. In Section IV, we develop a new cross-layer framework to analyze the sum rates and QoS performance. In Section V, we apply the framework to multiuser scenarios and derive the approximation of effective capacities under the RR and the max-C/I scheduling policies. In Section VI, we build a simulation platform to validate the accuracy of

In this work, we develop a cross-layer framework for capacity analysis in multiuser UDNs with Cell DTx.

our proposed framework. Section VII summarizes our work.

II. System Model

2.1 System architecture

A system model of a multiuser UDN with Cell DTx is shown in figure 1. The network consists of N SBSs and each SBS serves multiple user equipments (UEs) in a shared channel. The set of SBSs is denoted by $\mathcal{N}=\{1,2,\cdots,N\}$, where N is the number of SBSs. The set of UEs in SBS n ($n\in\mathcal{N}$) is denoted by $\mathcal{J}_n=\{1,2,\cdots,J_n\}$, where J_n is the total number of corresponding UEs.

Each UE is assigned an infinite-sized buffer in its associated SBS. SBSs apply a specific scheduling policy to allocate the shared channel resource among multiple UEs [21]. In this paper, we consider two scheduling policies, namely, the round robin (RR) and the max-C/I scheduling policies.

All SBSs use Cell DTx, i.e., each SBS has two modes, namely an idle mode and an active mode. In the idle modes, the elements for transmission such as the power amplifier are switched off to reduce interference and save energy [22]. In this paper, we consider the dynamic Cell DTx process, i.e., the SBS can be dynamically switched to an idle or active mode depending on whether there is data to transmit at any slot [23]. If the buffer of the scheduled UE is empty and there is no data arrival at this slot, the SBS switches to the idle mode; otherwise, it stays in the active mode for the target UE's data transmission [20]. Figure 2 illustrates the transition between the two modes.

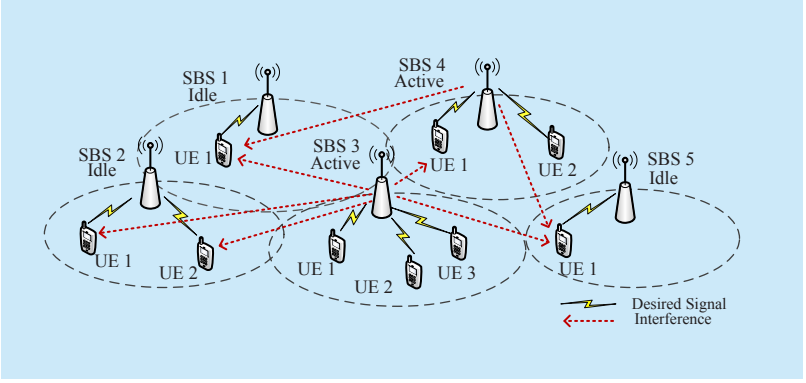

Fig. 1. *An example of the system model consisting five SBSs and corresponding UEs. SBS 3 and 4 are active to transmit the data while SBS 1, 2 and 5 are in the idle mode.*

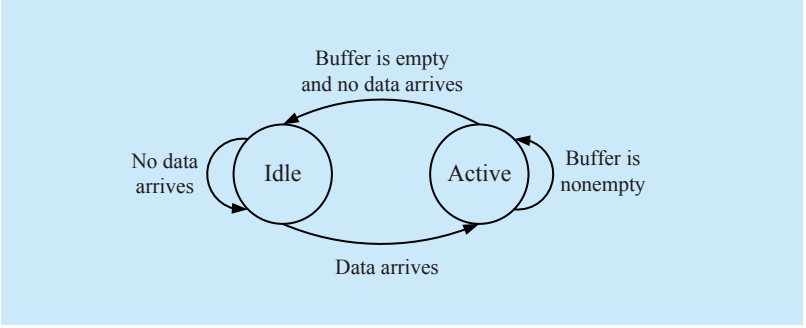

Fig. 2. *Transition between two modes of a SBS with Cell DTx.*

2.2 Inter-cell interference modeling

In order to analyze a fine-grained performance of individual link, we first consider UEs' signal-to-interference-plus-noise ratio (SINR) distribution in SBS $n\left(n\in\mathcal{N}\right)$ [24]. We assume that the wireless channels experience block Rayleigh fading and channel conditions of UEs in SBS n are mutually independent. Let $\mathcal{M}$ denotes the set of other active SBSs except SBS n at a given slot. The average received power of UEs in SBS n is assumed to be equal and is denoted by $P_{n,n}$; the average interference power received by UEs in SBS n from SBS $i\left(i\in\mathcal{M}\right)$ is assumed to be equal and is denoted by $P_{i,n}$. Therefore, UEs in SBS n have the same SINR distribution. The received SINR of UE $j\left(j\in\mathcal{J}_n\right)$ in SBS n can be written as

$$\gamma_{n,j}=\frac{P_{n,n}\,|\,H_{n,n,j}\,|^2}{\sum_{i\in\mathcal{M}}P_{i,n}\,|\,H_{i,n,j}\,|^2+N_0B},\qquad(1)$$

where N_0 is the noise spectral density, B is the channel bandwidth, $H_{i,n,j}$ is the Rayleigh fading coefficient between SBS i and UE j in SBS n and $\left|H_{i,n,j}\right|^2$ is the channel gain which is exponentially distributed with unit mean, $\sigma^2=N_0B$ is the power of the additive white

Gaussian noise.

The service $S_{n,j}[k](k=1,2,3\cdots)$ is the amount of bits that SBS n can transmit to UE j at slot k. The service sequence $S_{n,j}[1], S_{n,j}[2], \cdots$ are independent and identically distributed (i.i.d.) random variables (RVs) identical to a RV $S_{n,j}$. According to Shannon's theorem, $S_{n,j}$ is a function of the bandwidth B, the duration of a slot T_s and the SINR $\gamma_{n,j}$:

$$S_{n,j} = BT_s \log_2(1+\gamma_{n,j}). \quad (2)$$

Because UEs in SBS n have the same SINR distribution and (2) holds, their services $S_{n,1}, S_{n,2}, \cdots, S_{n,J_n}$ follow an identical distribution.

2.3 Traffic modeling

We follow the work [20] and make the following assumptions for UEs' traffic characters in SBS $n(n \in \mathcal{N})$:

1) The traffic arrival of UE j in SBS n, $A_{n,j}[1], A_{n,j}[2], \cdots$ are i.i.d. RVs identical to a RV $A_{n,j}$;

2) The traffic arrivals of UEs in SBS n confirm to a same Bernoulli process with a data arrival probability p_n ($p_n \in (0,1]$);

3) The traffic arrivals of UEs in SBS n in every slot follow a same exponential distribution. The average arrival size per slot is denoted by L_n;

Based on the above assumptions, the traffic arrivals of UEs in SBS n, $A_{n,1}, A_{n,2}, \cdots, A_{n,J_n}$ are i.i.d. RVs identical to a RV A_n. The probability distribution function (PDF) of A_n is

$$f_{A_{n,j}}(a) = f_{A_n}(a) = \begin{cases} p_n \frac{1}{L_n} e^{-\frac{a}{L_n}} & (a>0) \\ 1-p_n & (a=0) \end{cases}. \quad (3)$$

$\mu_{n,j}$ is the average arrival rate of UE j in SBS n. Based on (3), $\mu_{n,1}, \mu_{n,2}, \cdots, \mu_{n,J_n}$ equal a single value μ_n:

$$\mu_{n,j} = \mu_n = L_n p_n / T_s. \quad (4)$$

III. Preliminaries: One-Dimensional Effective Capacity Model

In the context of the traditional one-dimensional effective capacity model, the arrival and service rates of UE $j(j \in \mathcal{J}_n)$ in SBS $n(n \in \mathcal{N})$ can be characterized by their effective bandwidth $\alpha_{n,j}^{(b)}(u_{n,j})$ and effective capacity $\alpha_{n,j}^{(c)}(u_{n,j})$ [20]:

$$\alpha_{n,j}^{(b)}(u_{n,j}) = \frac{\Lambda_{A_{n,j}}(u_{n,j})}{u_{n,j}T_s} = \frac{1}{u_{n,j}T_s}\log\left(\frac{p_n}{1-u_{n,j}L_n}+1-p_n\right), \quad (5)$$

$$\alpha_{n,j}^{(c)}(u_{n,j}) = -\frac{\Lambda_{S_{n,j}}(-u_{n,j})}{u_{n,j}T_s}, \quad (6)$$

where $u_{n,j}$ is the QoS exponent, $\Lambda_{A_{n,j}}(u_{n,j})$ and $\Lambda_{S_{n,j}}(-u_{n,j})$ are the log-moment generating functions of $A_{n,j}$ and $S_{n,j}$, respectively. Let $C_{n,j}$ denotes the service rate of UE j in SBS n. By adopting the work by Soret et. al. [25], (6) can be approximated by a simplified form:

$$\alpha_{n,j}^{(c)}(u_{n,j}) \approx \mathrm{E}[C_{n,j}] - \frac{\mathrm{Var}(C_{n,j})T_s}{2}u_{n,j}, \quad (7)$$

where E[•] is an expectation operator and Var(•) is a variance operator.

Corollary 3.1: when $u_{n,j} \to 0$, the effective capacity of UE j in SBS n approaches to the ergodic capacity $\mathrm{E}[C_{n,j}]$. Meanwhile, the sum rate of SBS n, C_{phy_n} can be given by

$$C_{phy\_n} = J_n \mathrm{E}[C_{n,j}]. \quad (8)$$

If there is a unique QoS exponent $u_{n,j}^* > 0$ that satisfies

$$\alpha_{n,j}^{(b)}(u_{n,j}^*) = \alpha_{n,j}^{(c)}(u_{n,j}^*), \quad (9)$$

then the complementary cumulative distribution function (CCDF) of the quene length $Q_{n,j}$ can be approximated by [26]

$$P(Q_{n,j} > B_{n,j}) \approx p_b^{n,j} e^{-u_{n,j}^* B_{n,j}}, \quad (10)$$

where $P(\cdot)$ is the probability of an event, $B_{n,j}$ is a queue length bound, $p_b^{n,j}$ is the nonempty

buffer probability of the queue. According to the work [26]:

$$p_b^{n,j} \approx 1 - u_{n,j}^* L_n. \tag{11}$$

Denote $D_{n,j}$ as the steady-state delay experienced by a flow of UE j in SBS n. According to the work [27], $D_{n,j}$ is a RV and its CCDF can be approximated as

$$P(D_{n,j} > t_{n,j}) \approx p_b^{n,j} e^{-u_{n,j}^* \alpha_{n,j}^{(b)}(u_{n,j}^*) t_{n,j}} \approx \left(1 - \frac{p_n u_{n,j}^* L_n}{1 - u_{n,j}^* L_n + p_n u_{n,j}^* L_n}\right)^{\frac{t_{n,j}}{T_s}+1}, \tag{12}$$

where $t_{n,j}$ is a delay bound.

Corollary 3.2: The average delay experienced by a flow of UE j in SBS n, $\mathrm{E}\left[D_{n,j}\right]$ is given by

$$\mathrm{E}[D_{n,j}] = \int_0^{+\infty} P(D_{n,j} > t_{n,j})\, dt_{n,j} = \frac{1 - u_{n,j}^* L_n}{p_n u_{n,j}^* L_n}. \tag{13}$$

Proof: It can be implied from (12) that the delay $D_{n,j}$ follows a geometric distribution. Therefore, its mean $\mathrm{E}\left[D_{n,j}\right]$ can be derived according to [28].

Algorithm 1. An iterative bisection search algorithm to solve (17).

Algorithm algo()

1. Given $L_1, \cdots, L_N$, initialize the upper bound $\mathbf{up} = \left[\frac{1}{L_1}, \cdots, \frac{1}{L_N}\right]$, the lower bound $\mathbf{ul} = [0, \cdots, 0]$, the tolerance ξ (e.g., $\xi = 10^{-5}$)
2. Determine $f_n(\mathbf{u}) = \alpha_{n,j}^{(c)}(\mathbf{u}) - \alpha_{n,j}^{(b)}(u_n)$
3. Suppose $P_{idle\_i} = 1 (i \in \mathcal{M})$, obtain $u_n^{(0)}$ by solving $f_n\left(u_n^{(0)}\right) = \alpha_{n,j}^{(c)}\left(u_n^{(0)}\right) - \alpha_{n,j}^{(b)}\left(u_n^{(0)}\right) = 0$
4. Initialize $\mathbf{u}^{(0)} = \left[u_1^{(0)}, \cdots, u_N^{(0)}\right]$, update the upper bound $\mathbf{up}^{(0)} = \mathbf{u}^{(0)}$
5. Repeat
   for $i = 0 : maxIteration$ **do**
   proc 1
   end
6. Until $\left|f_n\left(\mathbf{u}^*\right)\right| \ll \xi, \forall n \in \mathcal{N}$

return $\mathbf{u}^*$

Procedure proc 1

1. $n = 1 + imodN$
2. $UL = 0$, $UP = \mathbf{up}^{(i)}[n]$, $\mathbf{up}^{(i+1)} = \mathbf{up}^{(i)}$, $\mathbf{u}^{(i+1)} = \mathbf{u}^{(i)}$
   while $\left|f_n\left(\mathbf{u}^{(i+1)}\right)\right| > \xi$ **do**
   if $f_n\left(\mathbf{u}^{(i+1)}\right) > 0$ **then**
   $UL = \mathbf{u}^{(i+1)}[n]$
   else
   $UP = \mathbf{u}^{(i+1)}[n]$
   end
3. $\mathbf{u}^{(i+1)}[n] = \frac{1}{2}(UL + UP)$
   end
4. $\mathbf{up}^{(i+1)}[n] = \mathbf{u}^{(i+1)}[n]$

return $\mathbf{u}^{(i+1)}, \mathbf{up}^{(i+1)}$

IV. Cross-Layer Analytical Framework for UDNS with Cell DTX

In order to analyze the sum rates and QoS performance of multiuser UDNs, we develop a new cross-layer framework for capacity analysis. In particular, the SBS idle probability is first studied in IV-A. Then we extend the traditional one-dimensional effective capacity model and develop a multidimensional model to derive sum rates of SBSs and UEs' effective capacity in IV-B. A new iterative bisection search algorithm is proposed and discussed in IV-C to find the unique QoS exponent vector and approximate the QoS performance.

4.1 Analysis of the SBS idle probability

As discussed in Section II-B and II-C, the arrival and service of UEs in SBS $n (n \in \mathcal{N})$ are both identically distributed, it can be implied from (5), (7) and (9) that the unique QoS exponents of UEs in SBS n, $u_{n,1}^*, u_{n,2}^*, \cdots u_{n,J_n}^*$ are equal to u_n^*:

$$u_{n,j}^* = u_n^* \ (j \in \mathcal{J}_n). \tag{14}$$

Based on (11) and (14), the nonempty buffer probability of the queues in SBS n, $p_b^{n,1}, p_b^{n,2}, \cdots p_b^{n,J_n}$ are equal to p_b^n:

$$p_b^{n,j} = p_b^n \ (j \in \mathcal{J}_n). \tag{15}$$

The idle probability of SBS n at slot k is denoted by $P_{idle\_n}[k]$. It is equivalent to 1) the

probability that the scheduled queue is empty meanwhile 2) no data arrives at the queue during slot k [25]. According to (10) and (15), the queues in SBS n follow a same distribution. Therefore, the probability that the scheduled queue is empty equals to $1-p_b^n$ at each slot. Moreover, the probability that no data arrives at each slot equals to $1-p_n$. Therefore, $P_{idle\_n}[1], P_{idle\_n}[2], \cdots$ are i.i.d. RVs identical to a RV P_{idle_n}. Since these two events are mutually independent, P_{idle_n} can be written as a product of the empty buffer probability $1-p_b^n$ and non-arrival probability $1-p_n$:

$$P_{idle\_n} = (1-p_b^n)(1-p_n) \approx u_n^* L_n (1-p_n). \quad (16)$$

4.2 Multidimensional effective capacity model

According to the discussion made in Section II-B and IV-A, the interference experienced by UE $j\left(j \in \mathcal{J}_n\right)$ in SBS $n\left(n \in \mathcal{N}\right)$ is a function of the idle probability of other SBSs, $P_{idle\_1}, \cdots, P_{idle\_n-1}, P_{idle\_n+1}, \cdots, P_{idle\_N}$. Therefore, the mean and the variance of the service rate, $\mathrm{E}\left[C_{n,j}\right]$ and $\mathrm{Var}\left(C_{n,j}\right)$ both are functions of $u_1, \cdots, u_{n-1}, u_{n+1}, \cdots, u_N$. From (7), it can be implied that the effective capacity of UE j in SBS n, $\alpha_{n,j}^{(c)}\left(u_{n,j}\right)$ is a function of all the QoS exponents $u_1, \cdots, u_N$.

Proposition 4.1: According to (9), the key of analyzing the sum rates and QoS performance is to find the unique QoS exponents $u_1^*, \cdots, u_N^* > 0$ that satisfy the following equations:

$$\begin{cases} \alpha_{1,j}^{(c)}(\mathbf{u}^*) = \alpha_{1,j}^{(b)}(u_1^*) \\ \alpha_{2,j}^{(c)}(\mathbf{u}^*) = \alpha_{2,j}^{(b)}(u_2^*) \\ \cdots \\ \alpha_{N,j}^{(c)}(\mathbf{u}^*) = \alpha_{N,j}^{(b)}(u_N^*) \end{cases}, \quad (17)$$

where $\mathbf{u}^* = [u_1^*, \cdots, u_N^*]$ is the unique QoS exponent vector. Eq. (17) can be solved by numerical methods, such as Newton's method. However, calculating the Jacobian matrix of (17) when using Newton's method is complicated and time-consuming. Therefore, we develop an efficient algorithm that iteratively applies bisection search to solve (17), which is expressed in pseudocode in Algorithm 1.

4.3 Convergence of algorithm 1

The following proposition and lemmas reveal the key properties of the effective capacity, which is the basic of Algorithm 1:

Proposition 4.2: When $\mathbf{u} \setminus u_n$ is fixed, there must be an unique QoS exponent u_n^* that satisfies $\alpha_{n,j}^{(c)}\left(u_n^*\right) = \alpha_{n,j}^{(b)}\left(u_n^*\right)$, where $\mathbf{u} \setminus u_n = [u_1, \cdots, u_{n-1}, u_{n+1}, \cdots, u_N]$ collects all other QoS exponents.

Proof: According to *Corollary 3.1*, when $u_n \to 0$, $\alpha_{n,j}^{(c)}\left(u_n\right)$ approaches to the ergodic capacity $\mathrm{E}\left[C_{n,j}\right]$. According to L'Hospital's rule, when $u_n \to 0$, $\alpha_{n,j}^{(b)}\left(u_n\right)$ approaches to the arrival rate $\mu_{n,j}$. Since the ergodic capacity should be larger than the arrival rate to guarantee the queueing stability, $\alpha_{n,j}^{(c)}\left(u_n\right) - \alpha_{n,j}^{(b)}\left(u_n\right) > 0$ when $u_n \to 0$. From (5) and (7), it can be implied that when $u_n \to \frac{1}{L_n}$, $\alpha_{n,j}^{(c)}\left(u_n\right)$ is expected to be a limited value while $\alpha_{n,j}^{(b)}\left(u_n\right)$ is expected to approach infinity. Therefore, $\alpha_{n,j}^{(c)}\left(u_n\right) - \alpha_{n,j}^{(b)}\left(u_n\right) < 0$ when $u_n \to \frac{1}{L_n}$. Moreover, according to work [12], $\alpha_{n,j}^{(c)}$ monotonically decreases with u_n while $\alpha_{n,j}^{(b)}$ monotonically increases with u_n. Therefore, there must be a unique QoS exponent u_n^* that satisfies $\alpha_{n,j}^{(c)}\left(u_n^*\right) = \alpha_{n,j}^{(b)}\left(u_n^*\right)$.

Lemma 4.3: When there is no interference between SBSs, the QoS exponent $u_n^{(0)}$ obtained by solving $f_n\left(u_n^{(0)}\right) = 0$ is the upper bound of u_n.

Proof: When there is no interference between the SBSs, UEs in SBS n have the best SINR performance. Since the idle probability of other SBS except SBS n can be regarded as 1, the effective capacity of UEs in SBS

n is independent of $\mathbf{u} \setminus u_n$. Therefore, according to *Proposition 4.2*, the upper bound of u_n (most stringent QoS requirements SBS n can support, in other words) can be obtained by finding the $u_n^{(0)}$ that satisfies $f_n\left(u_n^{(0)}\right) = \alpha_{n,j}^{(c)}\left(u_n^{(0)}\right) - \alpha_{n,j}^{(b)}\left(u_n^{(0)}\right) = 0$. This equation can be solved by bisection search with upper bound $\frac{1}{L_n}$ and lower bound zero.

Lemma 4.4: Denote (u_n) as the QoS exponent sequence of UE j in SBS n. The elements of (u_n) are the u_n approximations, $u_n^{(0)}, u_n^{(1)}, \cdots, u_n^{(k+1)}, \cdots$ in every N iterations. The sequence (u_n) is strictly monotonically decreasing with k, which means that $u_n^{(k)} > u_n^{(k+1)}$.

Proof: When take the interference from other SBSs into consideration to solve (17). In the n^{th} iteration, as the SINR performance degrades, the effective capacity of UE j in SBS n, $\alpha_{n,j}^{(c)}\left(\mathbf{u}^{(n-1)}\right)$ is smaller than the effective capacity in the initialization $\alpha_{n,j}^{(c)}\left(u_n^{(0)}\right)$. The effective bandwidth is independent of the interference, which means that $\alpha_{n,j}^{(b)}\left(\mathbf{u}^{(n-1)}\right) = \alpha_{n,j}^{(c)}\left(u_n^{(0)}\right)$. Therefore, we have $f_n\left(\mathbf{u}^{(n-1)}\right) < 0$. Since $\alpha_{n,j}^{(c)}$ monotonically decreases with u_n when $\mathbf{u} \setminus u_n$ is fixed, the $u_n^{(1)}$ that satisfies $f_n\left(\mathbf{u}^{(n)}\right) \ll \xi$ is smaller than $u_n^{(0)}$, where $\mathbf{u}^{(n)} = [u_1^{(1)}, \cdots u_n^{(1)}, u_{n+1}^{(0)}, \cdots u_N^{(0)}]$.

In the $(N+n)^{\text{th}}$ iteration, since $u_1^{(2)} < u_1^{(1)}, \cdots, u_{n-1}^{(2)} < u_{n-1}^{(1)}$, $\alpha_{n,j}^{(c)}\left(\mathbf{u}^{(N+n-1)}\right) < \alpha_{n,j}^{(c)}\left(\mathbf{u}^{(n)}\right)$ [19], where $\mathbf{u}^{(N+n-1)} = [u_1^{(2)}, \cdots u_{n-1}^{(2)}, u_n^{(1)}, \cdots u_N^{(1)}]$. However, since $\alpha_{n,j}^{(b)}\left(\mathbf{u}^{(N+n-1)}\right) = \alpha_{n,j}^{(b)}\left(\mathbf{u}^{(n)}\right)$, we have $f_n\left(\mathbf{u}^{(N+n-1)}\right) < 0$. When we fix $\mathbf{u} \setminus u_n$ and apply bisection search, the $u_n^{(2)}$ that satisfies $f_n\left(\mathbf{u}^{(N+n)}\right) \ll \xi$ is smaller than $u_n^{(1)}$, where $\mathbf{u}^{(N+n)} = [u_1^{(2)}, \cdots u_n^{(2)}, u_{n+1}^{(1)}, \cdots u_N^{(1)}]$.

In the $(kN+n)^{\text{th}}$ iteration, when fix $\mathbf{u} \setminus u_n$ and apply bisection search, the $u_n^{(k+1)}$ that satisfies $f_n\left(\mathbf{u}^{(kN+n)}\right) \ll \xi$ is smaller than $u_n^{(k)}$, where $\mathbf{u}^{(kN+n)} = [u_1^{(k+1)}, \cdots u_n^{(k+1)}, u_{n+1}^{(k)}, \cdots u_N^{(k)}]$.

It can be implied from *Lemma 4.4* that $u_n^{(k)} > u_n^{(k+1)}$, which means that the sequence (u_n) is strictly monotonically decreasing with k. Moreover, the sequence has a lower bound of zero [27]. Therefore, according to the monotone convergence theorem of the sequence [29], (u_n) can converge to the unique QoS exponent u_n^*, Algorithm 1 can converge to unique QoS exponent vector $\mathbf{u}^*$.

V. Examples: Effective Capacity of Multiuser UDNs with Cell DTX

In this section, we use the cross-layer analytical framework in Section IV-B to analyze the QoS performance of multiuser UDNs under the RR and the max-C/I scheduling policies. In particular, we first approximate the effective capacity of two-SBS single-user scenarios in V-A and then extend to N-SBS single-user scenarios in V-B. The effective capacity of N-SBS multiuser scenarios under the RR and the max-C/I scheduling policies are derived in V-C and D, respectively.

5.1 Effective capacity of two-SBS with single user

Suppose that the system consists of two SBSs, namely SBS 1 and SBS 2. Each SBS serves one single UE. We choose SBS 1 as the target SBS for the rest of the discussion. The SINR of the UE in SBS 1 may have two cases:

Case I: SBS 2 is in an idle mode and causes no interference to the UE in SBS 1 with probability $P_{idle\_2} \approx u_2^* L_2\left(1 - p_2\right)$. From (1), the UE's received SINR is

$$\gamma_{1,1}^{(1)} = \frac{P_{1,1} \mid H_{1,1,1} \mid^2}{\sigma^2}. \tag{18}$$

Because $\left|H_{1,1,1}\right|^2$ is exponentially distributed with unit mean, the PDF of the SINR is given by

$$f_{\gamma_{1,1}^{(1)}}(\gamma)=\frac{\sigma^2}{P_{1,1}}e^{-\frac{\sigma^2\gamma}{P_{1,1}}}. \quad (19)$$

Case II: SBS 2 is in a active mode and causes no interference to the UE in SBS 1 with probability $1-P_{idle\_2}\approx 1-u_2^*L_2(1-p_2)$. From (1), the UE's received SINR is

$$\gamma_{1,1}^{(2)}=\frac{P_{1,1}\mid H_{1,1,1}\mid^2}{P_{2,1}\mid H_{2,1,1}\mid^2+\sigma^2}. \quad (20)$$

Therefore, the PDF of the SINR is given by [20]

$$f_{\gamma_{1,1}^{(2)}}(\gamma)=\left(\frac{\sigma^2}{P_{1,1}+P_{2,1}\gamma}+\frac{P_{1,1}P_{2,1}}{(P_{1,1}+P_{2,1}\gamma)^2}\right)e^{-\frac{\sigma^2\gamma}{P_{1,1}}}. \quad (21)$$

By combing these two cases, the PDF of the UE's received SINR is a function of u_2:

$$f_{\gamma_{1,1}}(\gamma,u_2)=\left(P_{idle\_2}\frac{\sigma^2}{P_{1,1}}+(1-P_{idle\_2})\cdot\left(\frac{\sigma^2}{P_{1,1}+P_{2,1}\gamma}+\frac{P_{1,1}P_{2,1}}{(P_{1,1}+P_{2,1}\gamma)^2}\right)\right)e^{-\frac{\sigma^2\gamma}{P_{1,1}}}. \quad (22)$$

The cumulative distribution function (CDF) of the SINR is the integral of (22):

$$F_{\gamma_{1,1}}(\gamma,u_2)=1-\left(P_{idle\_2}+(1-P_{idle\_2})\frac{P_{1,1}}{P_{1,1}+P_{2,1}\gamma}\right)e^{-\frac{\sigma^2\gamma}{P_{1,1}}}. \quad (23)$$

Denote $C_{1,1}(u_2)$ as the instantaneous service rate of the UE. The mean of $C_{1,1}(u_2)$ is the ergodic capacity:

$$\begin{aligned}\mathrm{E}[C_{1,1}(u_2)]&=\int_0^{+\infty}B\log_2(1+\gamma)f_{\gamma_{1,1}}(\gamma,u_2)d\gamma\\&=\int_0^{+\infty}B\log_2(1+\gamma)\left(P_{idle\_2}\frac{\sigma^2}{P_{1,1}}+(1-P_{idle\_2})\cdot\left(\frac{\sigma^2}{P_{1,1}+P_{2,1}\gamma}+\frac{P_{1,1}P_{2,1}}{(P_{1,1}+P_{2,1}\gamma)^2}\right)\right)e^{-\frac{\sigma^2\gamma}{P_{1,1}}}d\gamma.\end{aligned} \quad (24)$$

The variance of $C_{1,1}(u_2)$ is

$$\mathrm{Var}(C_{1,1}(u_2))=\mathrm{E}[C_{1,1}{}^2(u_2)]-\mathrm{E}[C_{1,1}(u_2)]^2. \quad (25)$$

5.2 Effective capacity of N-SBS with single user

We proceed to consider N-SBS single-user scenarios. For SBS $n(n\in\mathcal{N})$, all other SBSs can either be in an idle or an active mode. Therefore, the number of possible interference cases is $2^{(N-1)}$. To derive UE's effective capacity in N-SBS single-user scenarios, we first make the following proposition:

Proposition 5.1: Let $\mathcal{N}\setminus n-\mathcal{M}$ and $\mathcal{N}\setminus n$ denote the set of idle SBSs and other SBSs except SBS n, respectively. The PDF of the UE's SINR can be given by

$$\begin{aligned}&f_{\gamma_{n,1}}(\gamma,\mathbf{u}\setminus u_n)=\\&\left(\sum_{\substack{\mathcal{M}\in\mathcal{P}(\mathcal{N}\setminus n)\\\mathcal{M}\neq\varnothing}}\left(\left(\prod_{i\in\mathcal{M}}(1-P_{idle\_i})\prod_{k\in\mathcal{N}\setminus n-\mathcal{M}}P_{idle\_k}\right)\right.\right.\\&\cdot\sum_{i\in\mathcal{M}}\left(\left(\prod_{t\in\mathcal{M}\setminus i}\frac{P_{i,n}}{P_{i,n}-P_{t,n}}\right)\frac{\sigma^2}{P_{i,n}\gamma+P_{n,n}}+\frac{P_{i,n}P_{n,n}}{(P_{i,n}\gamma+P_{n,n})^2}\right)\\&\left.\left.+\left(\prod_{q\in\mathcal{N}\setminus n}P_{idle\_q}\frac{\sigma^2}{P_{n,n}}\right)\right)e^{\frac{-\sigma^2\gamma}{P_{n,n}}},\end{aligned} \quad (26)$$

and the CDF of the UE's SINR is

$$\begin{aligned}&F_{\gamma_{n,1}}(\gamma,\mathbf{u}\setminus u_n)=\\&1-\left(\sum_{\substack{\mathcal{M}\in\mathcal{P}(\mathcal{N}\setminus n)\\\mathcal{M}\neq\varnothing}}\left(\left(\prod_{i\in\mathcal{M}}(1-P_{idle\_i})\prod_{k\in\mathcal{N}\setminus n-\mathcal{M}}P_{idle\_k}\right)\right.\right.\\&\left.\left.\cdot\frac{P_{n,n}^{|\mathcal{M}|}}{\prod_{i\in\mathcal{M}}(P_{i,n}\gamma+P_{n,n})}\right)+\prod_{q\in\mathcal{N}\setminus n}P_{idle\_q}\right)\cdot e^{\frac{-\sigma^2\gamma}{P_{n,n}}},\end{aligned} \quad (27)$$

where $\mathcal{P}(\mathcal{N}\setminus n)$ is the power set of the set $\mathcal{N}\setminus n$, which collects all possible interference cases. $|\mathcal{M}|$ is the cardinality of the set $\mathcal{M}$.

For a proof of *Proposition 5.1*, see Appendix A. Denote $C_{n,1}(\mathbf{u}\setminus u_n)$ as the instantaneous service rate of the UE in SBS n. The mean of $C_{n,1}(\mathbf{u}\setminus u_n)$ is the ergodic capacity:

$$\begin{aligned}&\mathrm{E}[C_{n,1}(\mathbf{u}\setminus u_n)]=\\&\int_0^{+\infty}B\log_2(1+\gamma)f_{\gamma_{n,1}}(\gamma,\mathbf{u}\setminus u_n)d\gamma.\end{aligned} \quad (28)$$

The variance of $C_{n,1}(\mathbf{u}\setminus u_n)$ is

$$\begin{aligned}&\mathrm{Var}(C_{n,1}(\mathbf{u}\setminus u_n))=\\&\mathrm{E}[C_{n,1}{}^2(\mathbf{u}\setminus u_n)]-\mathrm{E}[C_{n,1}(\mathbf{u}\setminus u_n)]^2.\end{aligned} \quad (29)$$

5.3 Effective capacity under the RR scheduling

Shown in figure 3, UEs in a same SBS are served in turns under the RR scheduling [5].

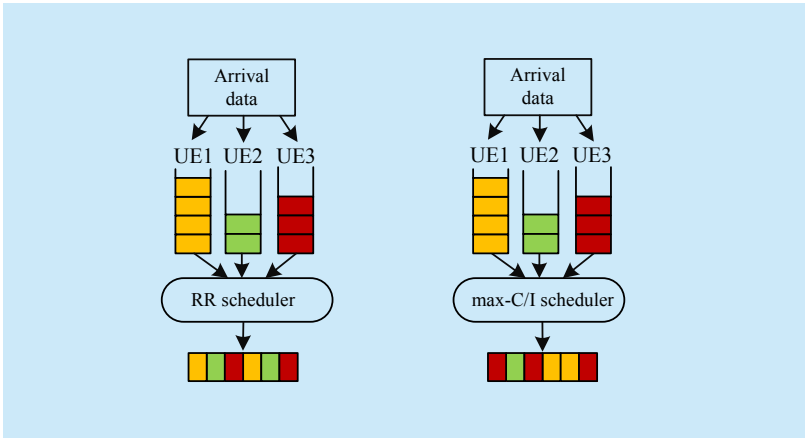

Fig. 3. *Link-layer scheduling process of RR and max-C/I.*

Table I. *Simulation parameters.*

Parameter	Value
Bandwidth, B	180kHz
Noise power density,N_0	-174dBm/Hz
Duration of a slot, T_S	1ms
Number of associated UEs, J_n	$J_1=3, J_2=2, J_3=3, J_4=3$
Mean value of the arrival data length, L_n	$L_1=2000, L_2=1000, L_3=1500, L_4=1200$
Data arrival probability, p_n	$p_1=p_2=p_3=p_4=0.1$
Average receive signal power, $P_{n,n}$	$P_{1,1}=P_{2,2}=P_{3,3}=P_{4,4}=-101.44$ dbm
Average interference power,$P_{i,n}$	$P_{1,2}=P_{2,1}=P_{3,4}=P_{4,3}=-119.44$ dbm, $P_{1,3}=P_{3,1}=P_{2,4}=P_{4,2}=-120.44$ dbm, $P_{1,4}=P_{4,1}=P_{2,3}=P_{3,2}=-119.94$ dbm,
Simulation time	10000 seconds

Define the received SINR of UE $j\left(j\in\mathcal{J}_n\right)$ in SBS $n\left(n\in\mathcal{N}\right)$ at slot $k\left(k=1,2,3\cdots\right)$ under the RR scheduling $\gamma_{n,j;\mathrm{RR}}\left[k\right]$ as follows:

$$\gamma_{n,j;\mathrm{RR}}[k]=\begin{cases}\gamma_{n,j}[k] & k \bmod J_n = j\\ 0 & k \bmod J_n \neq j\end{cases}. \quad (30)$$

Denote $C_{n,j;RR}\left(\mathbf{u}\setminus u_n\right)$ as the service rate of UE j in SBS n under the RR scheduling. Because SINR values are nonzero at certain slots (the j^{th} slots for every J_n slots), we make the following proposition:

Proposition 5.2: The mean and the variance of $C_{n,j;\mathrm{RR}}\left(\mathbf{u}\setminus u_n\right)$ are

$$\mathrm{E}[C_{n,j;\mathrm{RR}}(\mathbf{u}\setminus u_n)]=\frac{1}{J_n}\mathrm{E}[C_{n,1}(\mathbf{u}\setminus u_n)], \quad (31)$$

$$\mathrm{Var}(C_{n,j;\mathrm{RR}}(\mathbf{u}\setminus u_n))=\frac{1}{J_n}\mathrm{Var}(C_{n,1}(\mathbf{u}\setminus u_n))+\frac{J_n-1}{J_n^{\,2}}\mathrm{E}[C_{n,1}(\mathbf{u}\setminus u_n)]^2. \quad (32)$$

For a proof f *Proosition 5.2*, see Appendix B.

By substituting $\mathrm{E}\left[C_{n,j}\right]$ and $\mathrm{Var}\left(C_{n,j}\right)$ in (7) with (31) and (32), the effective capacity of UE j in SBS n under the RR scheduling can be approximated by

$$\alpha^{(c)}_{n,j;\mathrm{RR}}(\mathbf{u})\approx\frac{1}{J_n}\mathrm{E}[C_{n,1}(\mathbf{u}\setminus u_n)]-\frac{\left(\frac{1}{J_n}\mathrm{Var}(C_{n,1}(\mathbf{u}\setminus u_n))+\frac{J_n-1}{J_n^{\,2}}\mathrm{E}[C_{n,1}(\mathbf{u}\setminus u_n)]^2\right)T_s}{2}u_n. \quad (33)$$

5.4 Effective Capacity Under the Max-C/I Scheduling

Shown in figure 3, the UE with the instantaneously highest SINR is served under the max-C/I scheduling [5]. The received SINR of UE $j\left(j\in\mathcal{J}_n\right)$ in SBS $n\left(n\in\mathcal{N}\right)$ at slot $k\left(k=1,2,3\cdots\right)$ $\gamma_{n,j;\max}\left[k\right]$ is defined as [31]:

$$\gamma_{n,j;\max}[k]=\begin{cases}\gamma_{n,j}[k] & \gamma_{n,j}[k]>\gamma_{n,-j}[k]\\ 0 & \gamma_{n,j}[k]<\gamma_{n,-j}[k]\end{cases}, \quad (34)$$

where $\gamma_{n,-j}\left[k\right]=\max\limits_{m\in\mathcal{J}_n,m\neq j}\gamma_{n,m}\left[k\right]$ is the highest instantaneous SINR among UEs in SBS n except UE j. Because $\gamma_{n,-j}\left[k\right]$ are i.i.d. RVs identical to a RV $\gamma_{n,-j}$, $\gamma_{n,j;\max}\left[k\right]$ are i.i.d. RVs identical to a RV $\gamma_{n,j;\max}$. $C_{n,j;\max}\left(\mathbf{u}\setminus u_n\right)$ denotes the service rate of UE j in SBS n under the max-C/I scheduling and has the following property:

Proposition 5.3: The mean and the variance of $C_{n,j;\max}\left(\mathbf{u}\setminus u_n\right)$ are

$$\mathrm{E}[C_{n,j;\max}(\mathbf{u}\setminus u_n)]=\int_0^{+\infty}B\log_2(1+\gamma)F_{\gamma_{n,1}}(\gamma,\mathbf{u}\setminus u_n)^{J_n-1}f_{\gamma_{n,1}}(\gamma,\mathbf{u}\setminus u_n)d\gamma, \quad (35)$$

$$\mathrm{Var}(C_{n,j;\max}(\mathbf{u}\setminus u_n))=\mathrm{E}[C_{n,j;\max}{}^2(\mathbf{u}\setminus u_n)]-\mathrm{E}[C_{n,j;\max}(\mathbf{u}\setminus u_n)]^2, \quad (36)$$

where $F_{\gamma_{n,1}}\left(\gamma,\mathbf{u}\setminus u_n\right)$, $f_{\gamma_{n,1}}\left(\gamma,\mathbf{u}\setminus u_n\right)$ are given

by (27) and (26), respectively.

For a proof of *Proposition 5.3*, see Appendix C. By following the similar procedure in the analysis under the RR scheduling, the effective capacity of UE j in SBS n under the max-C/I scheduling can be approximated as

$$\alpha^{(c)}_{n,j;\max}(\mathbf{u}) \approx \mathrm{E}[C_{n,j;\max}(\mathbf{u}\setminus u_n)] - \frac{\mathrm{Var}(C_{n,j;\max}(\mathbf{u}\setminus u_n))T_s}{2}u_n. \quad (37)$$

Both Cell DTx and scheduling policies have no effect on the arrival process. Based on (5) the effective bandwidth of UE j in SBS n under both scheduling policies equal to

$$\alpha^{(b)}_{n,j;\mathrm{RR/max}}(u_n) = \frac{1}{u_n T_s}\log\left(\frac{p_n}{1-u_n L_n}+1-p_n\right). \quad (38)$$

We formulate the following nonlinear equations to find the unique QoS exponent vector $\mathbf{u}^*$ under the RR or the max-C/I scheduling policies:

$$\begin{cases} f_1(\mathbf{u}) = \alpha^{(c)}_{1,j;\mathrm{RR/max}}(\mathbf{u}) - \alpha^{(b)}_{1,j;\mathrm{RR/max}}(u_1) \\ \cdots \\ f_N(\mathbf{u}) = \alpha^{(c)}_{N,j;\mathrm{RR/max}}(\mathbf{u}) - \alpha^{(b)}_{N,j;\mathrm{RR/max}}(u_N) \end{cases}, \quad (39)$$

which could be solved by Algorithm 1 summarized in Section IV-B.

VI. Results and Discussions

A simulation platform is built based on a four-SBS system model described in Section II-A. The number of UEs served by SBS 1, 2, 3, 4 is set to be 3, 2, 3, 3, respectively. The bandwidth B is 180 kHz that equals an LTE resource block; the duration of a slot T_s is 1ms, which is a transmission time interval in LTE networks. The noise spectral density N_0 is set to -174 dBm/Hz. The average arrival rate of UEs in four SBSs are 200 Kbps, 100 Kbps, 150 Kbps and 120 Kbps, respectively. The average values of UEs' SINR in every SBS without the interference is 20 dB, which means that the average received signal power $P_{n,n}(n=1,2,3,4)$=-101.44 dBm. The average interference powers from other SBS $P_{i,n}(i\in\mathcal{N}\setminus n)$ are set according to the parameters in [19]. Table I lists all the simulation parameters used in our work.

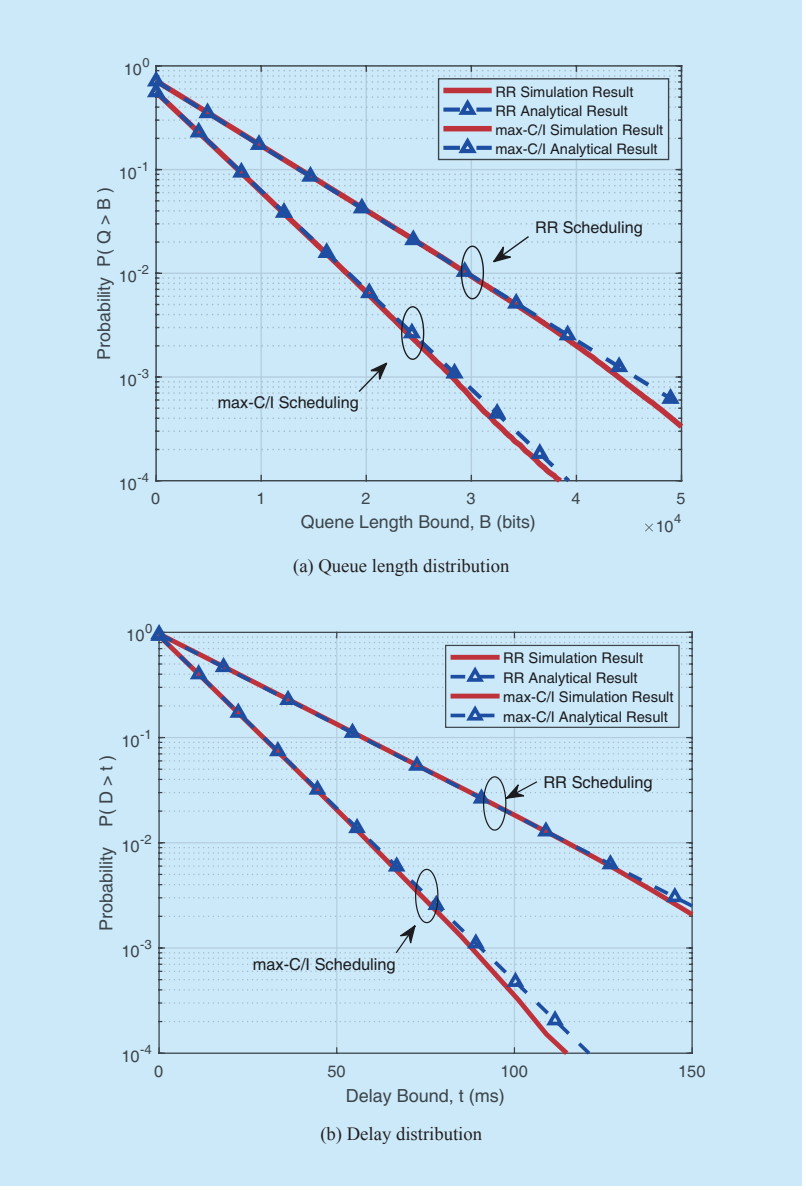

Fig. 4. *The queue length distribution $P(Q>B)$ and the delay distribution $P(D>t)$ of UE j in SBS 1 under the RR and the max-C/I scheduling policies.*

Figure 4(a) and (b) show simulation and analytical results of the queue length distribution $P(Q>B)$ and the delay distribution $P(D>t)$ of UE j in SBS 1 under the RR and the max-C/I scheduling policies, respectively. The unique QoS exponent vector $\mathbf{u}^*$ is numerically found by Algorithm 1 and the analytical results are calculated by (10) and (12). As illustrated in figure 4, the simulation and analytical results overlap with each other under both scheduling

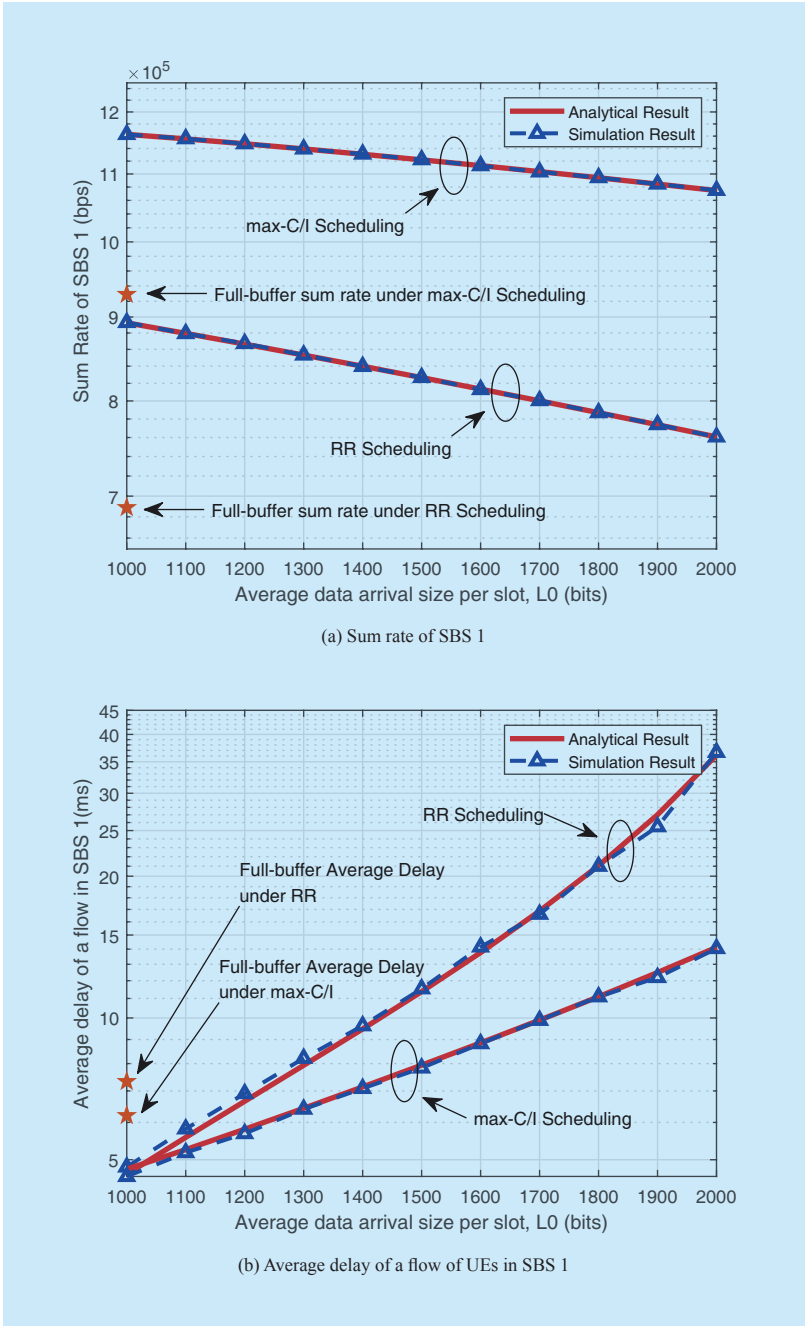

Fig. 5. *Sum rate of SBS 1 C_{phy_1} and average delay of a flow of UE j $\mathrm{E}\left[D_{1,j}\right]$ under the RR and the max-C/I scheduling policies with increasing average data arrival size.*

policies, indicating that our proposed framework can accurately approximate the effective capacity and QoS performance of multiuser UDNs with Cell DTx.

To study the improvement of Cell DTx, we further set L_1, L_2, L_3, L_4 to a same value L_0 and linearly increase L_0 from 1000 bits to 2000 bits, which means that the average arrival rates of UEs in the four SBSs increase from 100 Kbps to 200 Kbps.

Figure 5(a) shows the simulation and the analytical results of the sum rate C_{phy_1} of SBS 1 under the RR and the max-C/I scheduling policies, respectively. The sum rate of SBS 1 when assuming full-interference scenarios under the above two policies are starred as well. The analytical results with Cell DTx are calculated by (8) after obtaining the unique QoS exponent vector $\mathbf{u}^*$. The full-interference sum rate is obtained by setting $P_{idle\_n}\left(n=1,2,3,4\right)$ to 0, which means that all the SBSs are always transmitting and causing interference to others. As shown in figure 5 (a), when L_0 = 1000 bits, with Cell DTx SBS 1 has approximately 30% and 25% higher sum rates than those in full-buffer scenarios under the RR and the max-C/I, respectively. This is because that when the average arrival rate in each SBS is small, the SBSs are more likely to be idle with Cell DTx, which greatly reduce the ICI among SBSs. However, as the average arrival rates get larger, the interference caused by other active SBSs increases. As the SINR performance of UEs in SBS 1 degrades, the sum rate and idle probability of SBS 1 both decrease, which means $u_1^* \to 0$, Cell DTx scenario approaches to the full-buffer scenario. Therefore, the gap between the two scenarios narrows. Furthermore, we can see from figure 5(a) that SBS 1 is capable to obtain a larger sum rate under the max-C/I than the RR. This is because that the UE with the best channel condition is served at each slot under the max-C/I scheduling policy, a larger multiuser diversity is obtained to improve the sum rate and compensate the SINR performance degradation.

Figure 5(b) shows the simulation and the analytical results of the average delay $\mathrm{E}\left[D_{1,j}\right]$ of UE j in SBS 1 under the RR and the max-C/I scheduling policies, respectively. As shown in figure 5(b), when L_0 = 1000 bits, with Cell DTx SBS 1 has approximately 35% smaller average delays than those in full-buffer scenarios under both scheduling polices. However, $\mathrm{E}\left[D_{1,j}\right]$

increases with the average data arrival size gets larger. This is because that the queueing lengths of flows increase as the SINR performance of UE j degrades and service rate decreases.

VII. Conclusion

In this paper, we study the mathematical relationship among 1) the inter-cell interference, 2) the sum rates of SBSs, 3) scheduling policies and 4) QoS performance in multiuser UDNs with the Cell DTx. In particular, we develop a cross-layer analytical framework that consists of a new multidimensional effective capacity model and a new iterative bisection search algorithm. With this framework, we can approximate the sum rates and QoS performance under the round-robin and the max-C/I scheduling policies in multiuser scenarios. The simulation and analytical results are in good agreement for both policies, validating the accuracy of our proposed framework. Further extensions of our work might use this framework to optimize network operations such as power control and resource allocation.

Acknowledgements

This paper is supported by the National Science and Technology Major Project No. 2018ZX030110004, Beijing Natural Science Foundation (No. L182038), National Youth Top-notch Talent Support Program and the 111 Project of China (B16006).

Appendix A

Proof of Proposition 5.1

All possible sets of active SBSs map to all interference cases of the UE in SBS n. For a specific set of active SBS $\mathcal{M}$, the UE's SINR is given by (1)

$$\gamma_{n,1}=\frac{P_{n,n}\mid H_{n,n,1}\mid^2}{\sum_{i\in\mathcal{M}}P_{i,n}\mid H_{i,n,1}\mid^2+N_0B}, \tag{40}$$

where $\mathcal{M}\in\mathcal{P}(\mathcal{N}\setminus n),\mathcal{M}\neq\varnothing$. Let $X_{n,1}=P_{n,n}\left|H_{n,n,1}\right|^2$ denotes the received power of the UE in SBS n, $Y_{n,1}=I_{n,1}+\sigma^2=\sum_{i\in\mathcal{M}}P_{i,n}\left|H_{i,n,1}\right|^2+\sigma^2$ denotes the sum of the average received interference power and the noise. Suppose that $P_{i,n}\left(i\in\mathcal{M}\right)$ are different from each other. Therefore, $I_{n,1}$ is the sum of $|\mathcal{M}|$ exponential distributed variables with different means, whose distribution is a special case of the hypoexponential distribution. The PDF and CDF of $I_{n,1}$ are

$$f_{I_{n,1}}(g)=\sum_{i\in\mathcal{M}}\frac{1}{P_{i,n}}\left(\prod_{t\in\mathcal{M}\setminus i}\frac{P_{i,n}}{P_{i,n}-P_{t,n}}\right)e^{-\frac{g}{P_{i,n}}}, \tag{41}$$

$$F_{I_{n,1}}(g)=1-\sum_{i\in\mathcal{M}}\left(\prod_{t\in\mathcal{M}\setminus i}\frac{P_{i,n}}{P_{i,n}-P_{t,n}}\right)e^{-\frac{g}{P_{i,n}}}. \tag{42}$$

Note that the CDF of $I_{n,1}$ equals to 0 when substitute $g=0$ into (42), which means that

$$\sum_{i\in\mathcal{M}}\left(\prod_{t\in\mathcal{M}\setminus i}\frac{P_{i,n}}{P_{i,n}-P_{t,n}}\right)=1. \tag{43}$$

By substituting $g=y-\sigma^2$ into (41), we could obtain the PDF of $Y_{n,1}$

$$f_{Y_{n,1}}(y)=\sum_{i\in\mathcal{M}}\frac{1}{P_{i,n}}\left(\prod_{t\in\mathcal{M}\setminus i}\frac{P_{i,n}}{P_{i,n}-P_{t,n}}\right)e^{-\frac{(y-\sigma^2)}{P_{i,n}}}. \tag{44}$$

Because $X_{n,1}$ follows an exponential distribution with mean $P_{n,n}$, the PDF of $\gamma_{n,1}$ can be derived according to [30]

$$\begin{aligned}&f_{\gamma_{n,1}}(\gamma\mid\mathcal{M})\\&=\sum_{i\in\mathcal{M}}\int_{\sigma^2}^{+\infty}y\frac{1}{P_{n,n}}e^{\frac{-\gamma y}{P_{n,n}}}\frac{1}{P_{i,n}}\left(\prod_{t\in\mathcal{M}\setminus i}\frac{P_{i,n}}{P_{i,n}-P_{t,n}}\right)e^{\frac{-\left(y-\sigma^2\right)}{P_{i,n}}}dy\\&=\sum_{i\in\mathcal{M}}\left(\prod_{t\in\mathcal{M}\setminus i}\frac{P_{i,n}}{P_{i,n}-P_{t,n}}\right)\left(\frac{\sigma^2}{P_{i,n}\gamma+P_{n,n}}+\frac{P_{i,n}P_{n,n}}{\left(P_{i,n}\gamma+P_{n,n}\right)^2}\right)e^{\frac{-\sigma^2y}{P_{n,n}}}.\end{aligned} \tag{45}$$

The CDF of $\gamma_{n,1}$ can derived by calculating the integral of (45) and simplified using (43)

$$\begin{aligned}&F_{\gamma_{n,1}}(\gamma\mid\mathcal{M})\\&=\sum_{i\in\mathcal{M}}\left(\prod_{t\in\mathcal{M}\setminus i}\frac{P_{i,n}}{P_{i,n}-P_{t,n}}\right)\left(1-\frac{P_{n,n}}{P_{i,n}\gamma+P_{n,n}}e^{\frac{-\sigma^2y}{P_{n,n}}}\right)\\&=1-\frac{P_{n,n}^{|\mathcal{M}|}}{\prod_{i\in\mathcal{M}}\left(P_{i,n}\gamma+P_{n,n}\right)}e^{\frac{-\sigma^2y}{P_{n,n}}}.\end{aligned} \tag{46}$$

The possibility of this specific set of active SBS $\mathcal{M}$ is given by

$$P_{\mathcal{M}} = \prod_{i\in\mathcal{M}}\left(1-P_{idle\_i}\right)\prod_{k\in\mathcal{N}\setminus n-\mathcal{M}} P_{idle\_k}. \quad (47)$$

When $\mathcal{M}=\varnothing$, there is no other active SBS that causes interference to the UE in SBS n. We could derive the PDF and CDF of $\gamma_{n,1}$ in this case:

$$f_{\gamma_{n,1}}(\gamma,\mathbf{u}\setminus u_n) = \left(\prod_{q\in\mathcal{N}\setminus n} P_{idle\_q}\frac{\sigma^2}{P_{n,n}}\right)e^{\frac{-\sigma^2 y}{P_{n,n}}}, \quad (48)$$

$$F_{\gamma_{n,1}}(\gamma,\mathbf{u}\setminus u_n) = \left(\prod_{q\in\mathcal{N}\setminus n} P_{idle\_q}\right)\left(1-e^{\frac{-\sigma^2 y}{P_{n,n}}}\right). \quad (49)$$

Considering all the $2^{(N-1)}$ possible interference cases, the PDF and CDF of the SINR of the UE in SBS n can be given by

$$\begin{aligned} &f_{\gamma_{n,1}}(\gamma,\mathbf{u}\setminus u_n)\\ &=\left(\sum_{\substack{\mathcal{M}\in\mathcal{P}(\mathcal{N}\setminus n)\\ \mathcal{M}\neq\varnothing}}\left(\left(\prod_{i\in\mathcal{M}}(1-P_{idle\_i})\prod_{k\in\mathcal{N}\setminus n-\mathcal{M}} P_{idle\_k}\right)\right.\right.\\ &\left.\cdot\sum_{i\in\mathcal{M}}\left(\left(\prod_{t\in\mathcal{M}\setminus i}\frac{P_{i,n}}{P_{i,n}-P_{t,n}}\right)\frac{\sigma^2}{P_{i,n}\gamma+P_{n,n}}+\frac{P_{i,n}P_{n,n}}{(P_{i,n}\gamma+P_{n,n})^2}\right)\right)\\ &\left.+\left(\prod_{q\in\mathcal{N}\setminus n} P_{idle\_q}\frac{\sigma^2}{P_{n,n}}\right)\right)e^{\frac{-\sigma^2\gamma}{P_{n,n}}}, \end{aligned} \quad (50)$$

$$\begin{aligned} &F_{\gamma_{n,1}}(\gamma,\mathbf{u}\setminus u_n)\\ &=1-\left(\sum_{\substack{\mathcal{M}\in\mathcal{P}(\mathcal{N}\setminus n)\\ \mathcal{M}\neq\varnothing}}\left(\left(\prod_{i\in\mathcal{M}}(1-P_{idle\_i})\prod_{k\in\mathcal{N}\setminus n-\mathcal{M}} P_{idle\_k}\right)\right.\right.\\ &\left.\left.\cdot\frac{P_{n,n}^{|\mathcal{M}|}}{\prod_{i\in\mathcal{M}}\left(P_{i,n}\gamma+P_{n,n}\right)}\right)+\prod_{q\in\mathcal{N}\setminus n} P_{idle\_q}\right)e^{\frac{-\sigma^2\gamma}{P_{n,n}}}. \end{aligned} \quad (51)$$

Appendix B

Proof of Proposition 5.2

According to (2) and (30), only the service rates at the j^{th} slots for every J_n slots are non-zero. Therefore, the mean of $C_{n,j;\mathrm{RR}}(\mathbf{u}\setminus u_n)$ is

$$\begin{aligned} \mathrm{E}[C_{n,j;\mathrm{RR}}(\mathbf{u}\setminus u_n)] &= \lim_{N\to\infty}\frac{1}{N}\sum_{k=1}^{N} C_{n,j;\mathrm{RR}}(\mathbf{u}\setminus u_n)[k]\\ &= \frac{1}{J_n}\mathrm{E}[C_{n,1}(\mathbf{u}\setminus u_n)]. \end{aligned} \quad (52)$$

According to the definition, the variance of $C_{n,j;\mathrm{RR}}(\mathbf{u}\setminus u_n)$ is (53) shown in the bottom at this page.

where

$$x = j+mJ_n, m=0,1,2,\cdots \quad (54)$$

Denote $\Delta C_{n,j;\mathrm{RR}}(\mathbf{u}\setminus u_n)[x] = C_{n,j;\mathrm{RR}}(\mathbf{u}\setminus u_n)[x] - \mathrm{E}\left[C_{n,1}(\mathbf{u}\setminus u_n)\right]$. Because

$$\lim_{N\to\infty}\sum_{m=0}^{N/J_n}\Delta C_{n,j;\mathrm{RR}}(\mathbf{u}\setminus u_n)[x] = 0, \quad (55)$$

$$\begin{aligned} &\lim_{N\to\infty}\frac{1}{N}\sum_{m=0}^{N/J_n}\left(\Delta C_{n,j;\mathrm{RR}}(\mathbf{u}\setminus u_n)[x]\right)^2\\ &=\frac{1}{J_n}\mathrm{Var}\left(C_{n,1}(\mathbf{u}\setminus u_n)\right)^2, \end{aligned} \quad (56)$$

then the variance of $C_{n,j;\mathrm{RR}}(\mathbf{u}\setminus u_n)$ is (57) shown in the bottom at this page.

Appendix C

Proof of Proposition 5.3

The PDF of $\gamma_{n,j;\max}$ can be found in the work

$$\begin{aligned} &\mathrm{Var}(C_{n,j;\mathrm{RR}}(\mathbf{u}\setminus u_n)) = \lim_{N\to\infty}\frac{1}{N}\sum_{k=1}^{N}(C_{n,j;\mathrm{RR}}(\mathbf{u}\setminus u_n)[k]-\mathrm{E}[C_{n,j;\mathrm{RR}}(\mathbf{u}\setminus u_n)])^2\\ &=\lim_{N\to\infty}\frac{1}{N}\left(\frac{(J_n-1)N}{J_n}\mathrm{E}[C_{n,j;\mathrm{RR}}(\mathbf{u}\setminus u_n)]^2+\sum\left(C_{n,j;\mathrm{RR}}(\mathbf{u}\setminus u_n)[x]-\mathrm{E}[C_{n,j;\mathrm{RR}}(\mathbf{u}\setminus u_n)]\right)^2\right), \end{aligned} \quad (53)$$

$$\begin{aligned} \mathrm{Var}(C_{n,j;\mathrm{RR}}(\mathbf{u}\setminus u_n)) &= \frac{J_n-1}{J_n}\left(\frac{\mathrm{E}[C_{n,1}(\mathbf{u}\setminus u_n)]}{J_n}\right)^2+\lim_{N\to\infty}\frac{1}{N}\sum_{m=0}^{N/J_n}\left(\Delta C_{n,j;\mathrm{RR}}(\mathbf{u}\setminus u_n)[x]+\frac{J_n-1}{J_n}\mathrm{E}[C_{n,1}(\mathbf{u}\setminus u_n)]\right)^2\\ &=\frac{J_n-1}{J_n^{\,3}}\mathrm{E}[C_{n,1}(\mathbf{u}\setminus u_n)]^2+\frac{1}{J_n}\mathrm{Var}(C_{n,1}(\mathbf{u}\setminus u_n))+\frac{(J_n-1)^2}{J_n^{\,3}}\mathrm{E}[C_{n,1}(\mathbf{u}\setminus u_n)]^2\\ &=\frac{1}{J_n}\mathrm{Var}(C_{n,1}(\mathbf{u}\setminus u_n))+\frac{J_n-1}{J_n^{\,2}}\mathrm{E}[C_{n,1}(\mathbf{u}\setminus u_n)]^2. \end{aligned} \quad (57)$$

[30]:

$$f_{\gamma_{n,j;\max}}(\gamma,\mathbf{u}\setminus u_n)=P\left(\gamma_{n,j}<\gamma_{n,-j}\right)\delta(\gamma)+F_{\gamma_{n,-j}}(\gamma,\mathbf{u}\setminus u_n)f_{\gamma_{n,j}}(\gamma,\mathbf{u}\setminus u_n), \tag{58}$$

where $\delta(\gamma)$ is the Dirac delta function, $f_{\gamma_{n,j}}$ is the PDF of SINR of UE j in SBS n in N-SBS single user scenarios. $F_{\gamma_{n,-j}}$ is the CDF of $f_{\gamma_{n,-j}}$. Based on the assumption that the channel conditions of UEs in a same SBS are mutually independent, $F_{\gamma_{n,-j}}$ can be derived according to order statistic [32]:

$$F_{\gamma_{n,-j}}(\gamma,\mathbf{u}\setminus u_n)=\prod_{m\in\mathcal{J}_n,\,m\neq j}F_{\gamma_{n,m}}(\gamma,\mathbf{u}\setminus u_n)=F_{\gamma_{n,1}}(\gamma,\mathbf{u}\setminus u_n)^{J_n-1}. \tag{59}$$

By substituting $f_{\gamma_{n,j}}(\gamma,\mathbf{u}\setminus u_n)$ and $F_{\gamma_{n,-j}}(\gamma,\mathbf{u}\setminus u_n)$ in (58) with (26) and (59), the PDF of $\gamma_{n,j;\max}$ can be written as

$$f_{\gamma_{n,j;\max}}(\gamma,\mathbf{u}\setminus u_n)=P\left(\gamma_{n,j}<\gamma_{n,-j}\right)\delta(\gamma)+F_{\gamma_{n,1}}(\gamma,\mathbf{u}\setminus u_n)^{J_n-1}f_{\gamma_{n,1}}(\gamma,\mathbf{u}\setminus u_n). \tag{60}$$

The mean of $C_{n,j;\max}(\mathbf{u}\setminus u_n)$ is

$$\begin{aligned}&\mathrm{E}[C_{n,j;\max}(\mathbf{u}\setminus u_n)]\\&\overset{(1)}{=}\int_0^{+\infty}B\log_2(1+\gamma)f_{\gamma_{n,j;\max}}(\gamma,\mathbf{u}\setminus u_n)d\gamma\\&\overset{(2)}{=}\int_0^{+\infty}B\log_2(1+\gamma)P\left(\gamma_{n,j}<\gamma_{n,-j}\right)\delta(\gamma)d\gamma\\&+\int_0^{+\infty}B\log_2(1+\gamma)F_{\gamma_{n,1}}(\gamma,\mathbf{u}\setminus u_n)^{J_n-1}f_{\gamma_{n,1}}(\gamma,\mathbf{u}\setminus u_n)d\gamma\\&\overset{(3)}{=}\int_0^{+\infty}B\log_2(1+\gamma)F_{\gamma_{n,1}}(\gamma,\mathbf{u}\setminus u_n)^{J_n-1}f_{\gamma_{n,1}}(\gamma,\mathbf{u}\setminus u_n)d\gamma.\end{aligned} \tag{61}$$

The 3^{rd} equality in follows due to the integral property of the Dirac delta function, i.e., the result of $\int_0^{+\infty}B\log_2(1+\gamma)P\left(\gamma_{n,j}<\gamma_{n,-j}\right)\delta(\gamma)d\gamma$ equals zero by substituting $\gamma=0$ into $B\log_2(1+\gamma)P\left(\gamma_{n,j}<\gamma_{n,-j}\right)$.

The variance of $C_{n,j;\max}(\mathbf{u}\setminus u_n)$ is

$$\mathrm{Var}(C_{n,j;\max}(\mathbf{u}\setminus u_n))=\mathrm{E}[{C_{n,j;\max}}^2(\mathbf{u}\setminus u_n)]-\mathrm{E}[C_{n,j;\max}(\mathbf{u}\setminus u_n)]^2. \tag{62}$$

Reference

[1] X. Ge, S. Tu, G. Mao, C. X. Wang, and T. Han, "5G Ultra-Dense Cellular Networks," *IEEE Wirel. Commun.*, vol. 23, no. 1, 2016, pp. 72-79.

[2] C. Yang, J. Li, Q. Ni, A. Anpalagan, and M. Guizani, "Interference-Aware Energy Efficiency Maximization in 5G Ultra-Dense Networks," *IEEE Trans. Commun.*, vol. 65, no. 2, 2017, pp. 728–739.

[3] J. Cheng, H. Koorapaty, P. Frenger, D. Larsson and S. Falahati, "Energy efficiency performance of LTE dynamic base station downlink DTX operation," *IEEE Veh. Technol. Conf.,* 2014.

[4] B. Soret, A. Domenico, S. Bazzi, N. Mahmood and K. Pedersen, "Interference Coordination for 5G New Radio," *IEEE Wirel. Commun.*, vol. 25, no. 3, 2018, pp. 131–137.

[5] E. Dahlman and J. Sko, 4G LTE/LTE-Advance for Mobile Broadband, Second Edition, Academic Press, 2014.

[6] Q. Cui, Z. Gong, W. Ni, Y. Hou, X. Chen, X. Tao, and P. Zhang, "Stochastic Online Learning for Mobile Edge Computing: Learningfrom Changes," *IEEE Commun. Mag.*, vol. 57, no. 3, 2019, pp. 63-69.

[7] R. Bonnefoi, C. Moy, and J. Palicot, "New macrocell downlink energy consumption minimization with cell DTx and power control," *IEEE Int. Conf. Commun.*, 2017.

[8] P. Chang and G. Miao, "Energy and Spectral Efficiency of Cellular Networks with Discontinuous Transmission," *IEEE Trans. Wirel. Commun.*, vol. 16, no. 5, 2017, pp. 2991–3002.

[9] G. Andersson, A. Vastberg, A. Devlic and C. Cavdar, "Energy efficient heterogeneous network deployment with cell DTx," *IEEE Int. Conf. Commun.*, 2016.

[10] H. Holtkamp, G. Auer, S. Bazzi and H. Haas, "Minimizing base station power consumption," *IEEE J. Sel. Areas Commun.*, vol. 32, no. 2, 2014, pp. 297–306.

[11] M. Polignano, D. Vinella, D. Laselva, "Power savings and QoS impact for VoIP application with DRX / DTX feature in LTE," *IEEE Veh. Technol. Conf.*, 2011.

[12] D. Wu and R. Negi, "Effective capacity: a wireless link model for support of quality of service," *IEEE Trans. Wirel. Commun.*, vol. 2, no. 4, 2003, pp. 630–643.

[13] Q. Cui, Y. Gu, W. Ni, and R. Liu, "Effective Capacity of Licensed-Assisted Access in Unlicensed Spectrum for 5G: From Theory to Application," *IEEE J. Sel. Areas Commun.*, vol. 35, no.8, 2017, pp. 1754–1767.

[14] T. Abrao, S. Yang, L. D. H. Sampaio, P. J. E. Jeszensky, and L. Hanzo, "Achieving maximum effective capacity in OFDMA networks operating under statistical delay guarantee," *IEEE Access*, vol. 5, 2017, pp. 14333–14346.

[15] Balasubramanian and S. L. Miller, "The effective capacity of a time division downlink scheduling system," *IEEE Trans. Commun.*, vol. 58, no. 1, 2010, pp. 73–78.
[16] Q. Wang, D. Wu and P. Fan, "Delay-constrained Optimal Link Scheduling In Wireless Sensor Networks," *IEEE Trans. Veh. Technol.*, vol. 59, no. 9, 2010, pp. 4564–4577.
[17] M. Weyres and J. Gross, "Effective Service Capacity Analysis of Interference-Limited Multi-Carrier Wireless Systems," *Proc. of the 2013 19th Eur. Wirel. Conf.*, 2013.
[18] Q. Cui, Y. Gu, W. Ni, X. Zhang, X. Tao, P. Zhang and R. Liu, "Preserving Reliability of Heterogeneous Ultra-Dense Distributed Networks in Unlicensed Spectrum," *IEEE Commun. Mag.*, vol. 56, no. 6, 2018, pp. 72–78.
[19] Y. Gu, Q. Cui, Y. Chen, W. Ni, X. Tao and P. Zhang, "Effective Capacity Analysis in Ultra-Dense Wireless Networks with Random Interference," *IEEE ACCESS*, vol. 6, 2018, pp. 19499–19508.
[20] B. Cai, Y. Chen, Q. Cui, X. Zhu, and Y. Yang, "Accurate Energy-Efficient Power Control for Uplink NOMA Systems under Delay Constraint," *2018 IEEE/CIC International Conference on Communications in China (ICCC)*, 2018, pp. 682-687.
[21] Q. Li, Y. Chen, Q. Cui, Y. Gu, and G. Mao, "Effective Capacity Analysis of Multiuser Ultra-Dense Networks with Cell DTx," *2018 24th Asia-Pacific Conference on Communications (APCC)*, 2018, pp. 21–27.
[22] R. Bonnefoi, C. Moy, H. Far`es, and J. Palicot, "Power Allocation for Minimizing Energy Consumption of OFDMA Downlink with Cell DTx," *24th International Conference on Telecommunications*, 2017.
[23] J. F. Cheng, H. Koorapaty, P. Frenger, D. Larsson, and S. Falahati, "Energy efficiency performance of LTE dynamic base station downlink DTX operation," *IEEE Veh. Technol. Conf.*, 2014.
[24] Q. Cui, X. Yu, Y. Wang, and M. Haenggi, "The SIR Meta Distribution in Poisson Cellular Networks With Base Station Cooperation," *IEEE Trans. Commun.,* vol. 66, no. 3, 2018, pp.1234-1249.
[25] Soret, M. Aguayo-Torres, and J. Entrambasaguas, "Capacity with explicit delay guarantees for generic sources over correlated Rayleigh channel," *IEEE Trans. Wirel. Commun.*, vol. 9, no. 6, 2010, pp. 1901–1911.
[26] Y. Chen and I. Darwazeh, "An Accurate Approximation of Delay with Nakagami-m Channels and Exponential Arrivals," *IEEE Global Communications Conference (GLOBECOM)*, 2015, pp. 1–6.
[27] J. Xu, Y. Chen, Q. Cui, and X. Tao, "Use of Two-Mode Transceiver Circuitry and Its Cross-Layer Energy Efficiency Analysis," *IEEE Commun. Lett.*, vol. 21, no. 9, 2017, pp. 2065–2068.
[28] Forbes, Statistical Distributions, Fourth edition, Wiley, 2010.
[29] J. Yeh, Real analysis: Theory of measure and integration, World Scientific, 2006.
[30] Papoulis and S.U. Pillai, Probability, random variables, and stochastic processes, Third Edition, McGraw-Hill, 2002.
[31] J. Perez, J. Ibanez, and I. Santamaria, "Exact closed-form expressions for the sum capacity and individual users' rates in broadcast ergodic rayleigh fading channels," *IEEE 8th Workshop on Signal Processing Advances in Wireless Communications*, 2007, pp. 1–5.
[32] H. A. David and H. N. Nagaraja, Order Statistics, Third Edition, Wiley, 2005.

Biographies

Qing Li, received the B.S. degree in Communication University of China, Beijing, China and is currently working toward a M.S. degree in Beijing University of Posts and telecommunications, Beijing, China. Her research interests include the interference modelling, quality-of-service analysis and resource management in ultra-dense networks.

Yu Chen, received the B.S. degree in electronic science and technology from the Beijing University of Posts and Telecommunications, Beijing, China, in 2006, and the Ph.D. degree in the department of electronic and electrical engineering from University College London, London, UK, in 2013. From 2013 to 2015, he was a research associate with the communications and information systems group, UCL. Since 2015, he has been with the School of the Information and Communication Engineering, Beijing University of Posts and Telecommunications, Beijing, where he is a Lecturer. His current research interests include end-to-end delay modeling, quality-of-service provisioning algorithm design, and cross-layer energy efficiency analysis.

Qimei Cui, received the B.E. and M.S. degrees in electronic engineering from Hunan University, Changsha, China, in 2000 and 2003, respectively, and the Ph.D. degree in information and communications engineering from the Beijing University of Posts and Telecommunications (BUPT), Beijing, China, in 2006. She has been a Full Professor with the School of Information and Communication Engineering, BUPT, since 2014. She was a Guest Professor with the Department of Electronic Engineering, University of Notre Dame, IN, USA, in 2016. Her main

research interests include broadband wireless communications and networking for 4G/5G, mobile computing and intelligent networking for M2M and IoT networks. She serves as a Technical Program Committee Member of several international conferences, such as the IEEE ICC, the IEEE Globecom, the IEEE WCNC, the IEEE PIMRC, the IEEE/CIC ICCC, the IEEE WCSP 2013 etc. She was a recipient of the Best Paper Award at APCC 2018, the Best Paper Award at the IEEE ISCIT 2012, the Best Paper Award at the IEEE WCNC 2014, the Honorable Mention Demo Award at the ACM MobiCom 2009, and the Young Scientist Award at the URSI GASS 2014. She serves as an Editor of Science China Information China, Guest Editor of the EURASIP Journal on Wireless Communications and Networking , International Journal of Distributed Sensor Networks and Journal of Computer Networks and Comm.

Yu Gu, received the B.S. degree in communication engineering from Dalian University of Technology, Dalian, China, in 2014, and the Ph.D. degree in information and communications engineering from the Beijing University of Posts and Telecommunications (BUPT), Beijing, China, in 2019. His main research interests include stochastic optimization theory, machine learning, large-scale distributed systems as well as their applications to 5G heterogeneous wireless networks.

Guoqiang Mao, was with the School of Electrical and Information Engineering, The University of Sydney. He joined the University of Technology Sydney, in 2014, as a Professor of wireless networking. He has published over 200 papers in international conferences and journals, which have been cited more than 7000 times. His research interests include intelligent transport systems, applied graph theory and its applications in telecommunications, the Internet of Things, wireless sensor networks, wireless localization techniques, and network performance analysis. He is a fellow of IET. He received the Top Editor Award for outstanding contributions to the IEEE TRANSACTIONS ON VEHICULAR TECHNOLOGY in 2011, 2014, and 2015. He is the Co-Chair of the IEEE Intelligent Transport Systems Society Technical Committee on Communication Networks. He has served as the chair, the co-chair, and a TPC member in a number of international conferences. He has been an Editor of the IEEE Transactions on Intelligent Transportation Systems since 2018, the IEEE Transactions on Wireless Communications since 2014, and the IEEE Transactions on Vehicular Technology since 2010.